



Propagation and remote sensing / Propagation et télédétection

Low-grazing angles scattering of electromagnetic waves from one-dimensional natural surfaces: Rigorous and approximate theories

Théories rigoureuses et approchées pour la diffraction des ondes électromagnétiques par des surfaces unidimensionnelles aux angles rasants

G. Soriano^{a,*}, P. Spiga^b, M. Saillard^c

^a Institut Fresnel, CNRS/Université Aix-Marseille, Domaine Universitaire de Saint-Jérôme, avenue Escadrille Normandie-Niemen, 13397 Marseille cedex 20, France

^b Pellenc Selective Technologies, 125, rue François Gernelle, BP 124, 84124 Perthuis cedex 4, France

^c LSEET CNRS/Université du Sud-Toulon Var, BP 20132, 83957 La Garde cedex, France

ARTICLE INFO

Article history:

Available online 20 February 2010

Keywords:

Remote sensing
Low-grazing angles
Natural surfaces

Mots-clés:

Télédétection
Angles rasants
Surfaces naturelles

ABSTRACT

We present a rigorous model, based on a specific boundary integral formalism for the wave scattering from rough, one-dimensional, dielectric or conducting surfaces at low-grazing incidence and scattering angles. Even though this so-called Grazing Method of Moment is, from a numerical cost point of view, independent of the incidence, it remains very numerically demanding. We thus propose an extrapolation technique for faster monostatic diagram computation, based on the theoretical behavior of the scattering amplitude at low-grazing angles. This technique is compared to the GMoM and to some approximate models, for surfaces with Gaussian spectrum as well as for sea surface.

© 2010 Académie des sciences. Published by Elsevier Masson SAS. All rights reserved.

RÉSUMÉ

Nous présentons un modèle rigoureux, fondé sur un formalisme intégral de frontière spécifique, pour la diffraction des ondes par des surfaces rugueuses unidimensionnelles, diélectriques ou conductrices, aux angles rasants. Même si cette méthode, appelée GMoM, est, en termes de coût numérique, indépendante de l'incidence, elle reste numériquement très exigeante. Nous proposons donc une technique d'extrapolation pour le calcul rapide des diagrammes monostatiques, fondée sur le comportement théorique de l'amplitude de diffraction aux angles rasants. Cette technique est comparée à la GMoM et à des modèles approchés, pour des surfaces à spectre gaussien ainsi que pour la surface de la mer.

© 2010 Académie des sciences. Published by Elsevier Masson SAS. All rights reserved.

1. Introduction

In this article we address the time-harmonic scattering of electromagnetic waves from rough surfaces at low-grazing incidence and scattering angles. The applications we have in mind mainly concern dielectric and conducting surfaces in optics, or soils and the sea surface at microwave frequencies. Low-grazing incidence is a difficult topic (see [1] for a dedicated special issue), but of particular interest in remote sensing. The normalized radar cross section (NRCS) becomes very small

* Corresponding author.

E-mail addresses: gabriel.soriano@fresnel.fr (G. Soriano), p.spiga@pellencst.com (P. Spiga), marc.saillard@lseet.univ-tln.fr (M. Saillard).

at low-grazing incidence, as most part of the incident power is scattered around the specular direction. Therefore, one can understand that designing an accurate model for this quantity is challenging.

The domain of validity of the most classical approximate models [2] has already been studied and more or less precisely defined (see for example [3–6]): height very small compared to the electromagnetic wavelength for the Small Perturbation Method (SPM), large curvature radii for the Kirchhoff-tangent plane Approximation (KA), small slope and moderate height for the first order of the Small Slope Approximation (SSA) [7], and so on. However, few models claim to be accurate at low-grazing angles (LGA) (see [8,9] for a perturbative approach at LGA), and the error at those angles, or even the order of magnitude of this error, cannot be predicted analytically.

The domain of validity of an approximation can be determined by comparison with reference data. These reference data may come from measurements or from the rigorous numerical solution of the scattering problem. For indoor facilities, in Optics or in the microwave range, the last degrees or tenths of degrees before grazing are out of range, due to the size of transmitters and receivers, while in outdoor measurements on natural surfaces, the rough surface and its environment is never fully controlled. Therefore, reliable numerical computations are of interest for the scientific community.

Numerical solutions of the rigorous scattering problem are now very mature for numerous one-dimensional and two-dimensional rough surfaces, except at LGA. As a matter of fact, one of the major point here is the so-called edge effect. As only a finite surface is sampled, the incident field has to be tapered to leave the edges of the sampled domain out of the beam. Gaussian beams are commonly used [10]. However, those tapered beams have a footprint on the surface that grows very fast when the incidence angle tends toward grazing. This problem remains in methods such as the Method of Ordered Multiple Interactions or the Forward–Backward approach [11,12].

In [13], we have presented a boundary integral method for the numerical solution of the rigorous problem of time-harmonic wave scattering from rough surfaces under grazing illumination. The rough surface is represented by a bounded perturbation of a plane and is enlightened by a plane wave. The integral equations are built on specific unknowns and right-hand sides that permit edge effects to be avoided. The integral operators involved are those commonly encountered in scattering, the scalar single- and double-layer and the vector Electric Field and Magnetic Field Integral Equation operators. This rigorous approach is called the Grazing Method of Moments (GMoM). It has been applied to two-dimensional perfectly conducting surfaces with Gaussian spectra to prove that the performances of some popular approximate methods, namely the SPM at first order and the SSA at first order, deteriorate drastically at backward scattering angles as the incidence goes to grazing.

Even though the numerical cost of the Grazing Method of Moments is independent of the incidence angle, it remains as a numerical method very RAM memory and CPU time demanding. In particular, bistatic diagrams for a given incidence angle are much less time-consuming than monostatic diagrams, for which the integral equation has to be solved for each angle. This is why, in this paper, we propose a method to extrapolate the results from the bistatic diagram at a given grazing incidence to predict monostatic diagrams over the whole range of grazing angles. It is proved through numerical computations over one-dimensional surfaces how these extrapolations compare with the GMoM for the two fundamental polarization cases.

The article is organized as follows. After this introduction comes the theoretical section where the principles of the GMoM are recalled and applied to electromagnetic scattering by one-dimensional surfaces. For both polarization cases, boundary integral equations are exhibited, either considering that the lower medium is a homogeneous (eventually lossy) dielectric medium, or applying the impedance approximation on the surface. Section 3 is devoted to the study of the theoretical behavior of the scattering amplitude at grazing incidence and/or grazing scattering angles. We derive an expression of the scattering amplitude that enforces this theoretical behavior when solving numerically the integral equations. The expressions of the coefficients required for extrapolating the scattering amplitude from grazing incidence and/or grazing angles is also deduced. In Section 4 about numerical results we present NRCS comparisons between the GMoM and its extrapolation from grazing. Two kinds of roughness with Gaussian spectra are investigated, with small height and in the resonant regime, respectively. Both dielectric and conducting surfaces encountered in Optics are studied. Furthermore, sea surfaces with Unified Ocean spectrum [14] at L-band microwave frequency are considered. Estimations from the KA, the SPM at first order and the SSA at first order, are also provided and compared to GMoM.

2. Boundary integral formalism

Let us consider a rough surface Γ invariant by translation along the y axis, described by $z = \eta(x)$, and separating air ($z > \eta(x)$) from a semi-infinite homogeneous medium. Γ is illuminated from air by a time-harmonic plane wave, with wavenumber $K = \omega/c$ and wavevector $\mathbf{k}^i = k_0 \hat{\mathbf{x}} - q_0 \hat{\mathbf{z}}$ in the xOz plane. The angle of incidence is defined as $\theta^i = (\mathbf{k}^i, -\hat{\mathbf{z}})$. The scattering problem is thus reduced to a two-dimensional problem, and the two fundamental cases of polarization, denoted by H (horizontal) and V (vertical) depending on whether the electric field \mathbf{E} or the magnetic field \mathbf{H} is along the y direction respectively, are uncoupled.

This problem is solved with the help of a rigorous boundary integral formalism combined with numerical solution of the integral equation. The boundary is assumed to be flat except in a bounded area $|x| < L/2$, to ensure a fast decreasing behavior of the unknown of the integral equation away from the rough area and thus make the computation tractable. The quantities are represented by their complex amplitude, assuming an $\exp(-i\omega t)$ time dependence.

If $u(x, z)$ is the y -component of the field of interest, that is $\mathbf{E}(\mathbf{r}) = u(x, z)\hat{\mathbf{y}}$ in the H polarization case and $\mathbf{H}(\mathbf{r}) = u(x, z)\hat{\mathbf{y}}$ for V polarization, let us define the scalar field $\psi(x, z)$ as

$$\psi = \begin{cases} u - (u^i + u^r) & z > \eta(x) \\ 0 & z < \eta(x) \end{cases} \quad (1)$$

where u^i and u^r denote the incident field and the field that would be reflected by the flat interface $z = 0$, respectively. u^r is thus a plane wave of wavevector $\mathbf{k}^r = k_0\hat{\mathbf{x}} + q_0\hat{\mathbf{z}}$. Its amplitude is given by the reflection coefficient that depends on the boundary condition. With $\eta' = \frac{d\eta}{dx}$ and $\hat{\mathbf{n}} = \frac{-\eta'\hat{\mathbf{x}} + \hat{\mathbf{z}}}{\sqrt{1+\eta'^2}}$ the normal unit vector directed toward air, $\psi^>$ and $\partial_n\psi^>$ denote the limit of the field and of its normal derivative, respectively, by approaching the surface from air.

In the upper half-space, ψ carries the sole contribution from surface roughness. For both polarization cases, ψ satisfies the same homogeneous Helmholtz equation in both half spaces, as well as an outgoing wave condition. Therefore Kirchhoff-Helmholtz formula applies and one gets, in the upper medium,

$$\psi(\mathbf{r}) = \int_{\Gamma} \{G(\mathbf{r}, \mathbf{r}')\partial_n\psi^>(\mathbf{r}') - \partial'_n G(\mathbf{r}, \mathbf{r}')\psi^>(\mathbf{r}')\} d\ell(\mathbf{r}') \quad (2)$$

where $G(\mathbf{r}, \mathbf{r}')$ and $\partial'_n G(\mathbf{r}, \mathbf{r}')$ denote the free space Green's function for vacuum and its normal derivative with respect to \mathbf{r}' , respectively. The two-dimensional Green's function in free space writes as $G(\mathbf{r}, \mathbf{r}') = \frac{-i}{4}H_0^+(K|\mathbf{r} - \mathbf{r}'|)$ where H_0^+ denotes the Hankel function of the first kind.

When \mathbf{r} tends toward Γ , one gets the integral equation for the unknowns $\psi^>$

$$\left(\frac{1}{2} + \mathcal{D}\right)\psi^> - \mathcal{S}\partial_n\psi^> = 0 \quad (3)$$

involving the single and double layer integral operators defined by

$$\mathbf{r} \in \Gamma, \quad \mathcal{S}\psi(\mathbf{r}) = \int_{\Gamma} G(\mathbf{r}, \mathbf{r}')\psi(\mathbf{r}') d\ell(\mathbf{r}'), \quad \mathcal{D}\psi(\mathbf{r}) = \int_{\Gamma} \partial'_n G(\mathbf{r}, \mathbf{r}')\psi(\mathbf{r}') d\ell(\mathbf{r}') \quad (4)$$

We now consider the field

$$\phi = \begin{cases} 0 & z > \eta(x) \\ u - u^t & z < \eta(x) \end{cases} \quad (5)$$

with u^t the field that would be transmitted through the flat interface $z = 0$ into the lower medium, of which relative permittivity is denoted by ε hereafter. With the same calculations as for ψ , one finds that the limit of the field $\phi^<$ and of its normal derivative $\partial_n\phi^<$ by approaching the surface from below satisfy the integral equation

$$\left(\frac{1}{2} - \mathcal{D}_\varepsilon\right)\phi^< + \mathcal{S}_\varepsilon\partial_n\phi^< = 0 \quad (6)$$

with \mathcal{S}_ε and \mathcal{D}_ε the single- and double-layer operators associated to the free space Green's function for the dielectric medium $G_\varepsilon(\mathbf{r}, \mathbf{r}') = \frac{-i}{4}H_0^+(K\sqrt{\varepsilon}|\mathbf{r} - \mathbf{r}'|)$.

Now, applying the boundary conditions $\phi^< = \psi^>$ and $\partial_n\phi^< = X\partial_n\psi^>$ with $X = 1$ in H polarization and $X = \varepsilon$ in the Vertical case, the scattering problem is cast into the system of two coupled integral equations

$$\begin{cases} \left(\frac{1}{2} + \mathcal{D}\right)\psi^> - \mathcal{S}\partial_n\psi^> = 0 \\ \left(\frac{1}{2} - \mathcal{D}_\varepsilon\right)\psi^> + \mathcal{S}_\varepsilon\partial_n\psi^> = \left(\frac{1}{2} - \mathcal{D}_\varepsilon\right)(u^t - u^i - u^r) + X\mathcal{S}_\varepsilon\left(\frac{1}{X}\partial_nu^t - \partial_nu^i - \partial_nu^r\right) \end{cases} \quad (7)$$

By definition, $u^t - u^i - u^r$ and $\frac{1}{X}\partial_nu^t - \partial_nu^i - \partial_nu^r$ vanish outside the rough region, that is for $|x| > L/2$. This ensures a fast decreasing behavior of the right-hand side of (7), and thus of the unknowns $\psi^>$ and $\partial_n\psi^>$ away from the rough area.

Integral equations (7) can be cast into a linear system using numerical techniques such as the Method of Moment (MoM), and sampling has thus to be performed at the smallest scale involved in the scattering process, including the wavelength. Therefore, this sampling becomes uncomfortable and numerically expensive when the relative permittivity of the lower medium is much larger than one, such as for conductors in Optics or wet soils and sea water at microwave frequencies. In those cases, a different boundary condition, although approximate, is preferred and found more reliable. It is often referred to as the impedance approximation, assuming a local relationship between the tangential components of the electric and magnetic fields

$$\mathbf{E}_t = -\hat{\mathbf{n}} \times (\hat{\mathbf{n}} \times \mathbf{E}) = [Z]\hat{\mathbf{n}} \times \mathbf{H} \quad (8)$$

where $[Z]$ is the local impedance matrix or dyad. The perfectly conducting limit corresponds to the particular case where $[Z] = 0$. For two-dimensional problems the impedance approximation leads to Robin boundary conditions, $\partial_n u = -iK \frac{Z_V}{Z_0} u$ in the Vertical polarization case and $\partial_n u = -iK \frac{Z_H}{Z_0} u$ in the Horizontal case, where $Z_0 = \sqrt{\frac{\mu_0}{\varepsilon_0}}$ is the impedance of air. For a rough surface $z = \eta(x)$ separating the air from a homogeneous medium with relative permittivity ε , Z_V and Z_H are functions of x , with the following series expansion with respect to the parameter $1/\sqrt{\varepsilon}$.

$$\frac{\sqrt{\varepsilon} Z_V}{Z_0} = \frac{Z_0}{\sqrt{\varepsilon} Z_H} = 1 + \frac{i}{2K\sqrt{\varepsilon}} \frac{\eta''}{(1 + \eta'^2)^{3/2}} + O\left(\frac{1}{\varepsilon}\right) \quad (9)$$

The two first terms are local and their use as boundary condition corresponds to the curved surface-impedance approximation [15]. Given definition (1), the Robin conditions become

$$\partial_n \psi^+ = -iK \frac{Z_V}{Z_0} \psi^+ - \phi_V, \quad \phi_V = \partial_n(u^i + u^r) + iK \frac{Z_V}{Z_0} (u^i + u^r) \quad (10)$$

$$\psi^+ = \frac{i}{K} \frac{Z_H}{Z_0} \partial_n \psi^+ - \phi_H, \quad \phi_H = (u^i + u^r) - \frac{i}{K} \frac{Z_H}{Z_0} \partial_n (u^i + u^r) \quad (11)$$

and Eq. (3) turns for both polarization cases to a single scalar unknown integral equation.

$$\left\{ \left(\frac{1}{2} + \mathcal{D} \right) + iK \mathcal{S} \frac{Z_V}{Z_0} \right\} \psi^+ = -\mathcal{S} \phi_V \quad (12)$$

$$\left\{ \frac{i}{K} \left(\frac{1}{2} + \mathcal{D} \right) \frac{Z_H}{Z_0} - \mathcal{S} \right\} \partial_n \psi^+ = \left(\frac{1}{2} + \mathcal{D} \right) \phi_H \quad (13)$$

Note that the reflected field u^r , $\partial_n u^r$ is to be build according to the Robin boundary condition, so that ϕ_V and ϕ_H are strictly zero outside the rough area.

3. Scattering amplitude, limits at grazing and extrapolation

From (1) and (2), and from Weyl's expansion, the scattering amplitude is defined for an incident plane wave of unit complex amplitude as

$$s^\pm(k, k_0) = \frac{1}{2\pi} \int_{\Gamma} \{ \mathbf{k}^\pm \cdot \hat{\mathbf{n}} \psi^> - i \partial_n \psi^> \} e^{-i\mathbf{k}^\pm \cdot \mathbf{r}} d\ell \quad (14)$$

in the direction indicated by wavevector $\mathbf{k}^\pm = (k, \pm q)$ satisfying $\mathbf{k}^2 = K^2$, $\Re q \geq 0$, $\Im m q \geq 0$ so that the scattered field at any point $\mathbf{r} = (x, z > \max \eta)$ is

$$u^d(\mathbf{r}) = u(\mathbf{r}) - u^i(\mathbf{r}) = u^r(\mathbf{r}) + \int_{\mathbb{R}} \frac{s^+(k, k_0)}{q} e^{i\mathbf{k}^+ \cdot \mathbf{r}} dk \quad (15)$$

while for any k ,

$$s^-(k, k_0) = 0 \quad (16)$$

which is the so-called extinction theorem. At this point, the behavior of scattering amplitude $s^+(k, k_0)$ at grazing scattering $q = K \cos \theta \rightarrow 0$ or incident $q_0 = K \cos \theta^i \rightarrow 0$ angles is not explicit. However, let us consider the difference $s^d = s^+ - s^-$ of which expression can be arranged into

$$s^d(k, k_0) = s^+(k, k_0) - s^-(k, k_0) \quad (17)$$

$$= \frac{1}{\pi} \int_{\Gamma} \left\{ \left(\frac{ik\eta' \psi^>}{\sqrt{1 + \eta'^2}} - \partial_n \psi^> \right) \sin(q\eta) + \frac{q\psi^>}{\sqrt{1 + \eta'^2}} \cos(q\eta) \right\} e^{-ikx} d\ell \quad (18)$$

$$= O(q) \quad (19)$$

In that case, it is obvious from s^- nullity that s^d is exactly equal to s^+ , and that the behavior of the scattering amplitude at grazing scattering angle is

$$s^+(k, k_0) = O(q) \quad (20)$$

Now, invoking Lorenz reciprocity for the scattering amplitude, $s^+(k, k_0) = s^+(-k_0, -k)$, we deduce that $s^+(k, k_0) = O(q_0)$. This behavior can also be proved while studying $u^t - u^i - u^r$ and $\frac{1}{x} \partial_n u^t - \partial_n u^i - \partial_n u^r$ at grazing incidence. Finally,

$$s^+(k, k_0) = O(q_0 q) \quad (21)$$

with immediate consequence that the incoherent scattering cross-section $\sigma(k, k_0) = \text{Var}(s^+(k, k_0)) = \langle |s^+(k, k_0) - \langle s^+(k, k_0) \rangle|^2 \rangle = O(q_0^2 q^2)$ and in the backscattering direction, $\sigma^b(k_0) = \sigma(-k_0, k_0) = O(q_0^4)$.

This important result for materials with finite permittivity can be extended to perfectly conducting metals, but for the H polarization case only [16].

It has been shown in [13] how the predictions of usual approximate rough surface scattering models deteriorate at grazing incidence and grazing backward scattering angles. As the use of rigorous computations is required, we investigate here a way to save computation time by taking benefit from the asymptotic behavior of the scattering amplitude exhibited in the previous section. With this aim we have to calculate the first term of the expansion of the scattering amplitude with respect to q and q_0 . Since $s^+(k, k_0) = O(q)$ as $q \rightarrow 0$, the limits

$$s_{10}^+(k_0) = \lim_{q \rightarrow 0} \frac{s^+(k, k_0)}{q} \quad (22)$$

are finite. Note that here are two such limits, $s_{10}^{+f}(k_0)$ for forward scattering $k > 0$ and $s_{10}^{+b}(k_0)$ for backward angles $k < 0$. For such grazing amplitudes the formula (18) becomes

$$s_{10}(k_0) = \frac{1}{\pi} \int_{\Gamma} \left\{ \frac{ik\eta\eta' + 1}{\sqrt{1 + \eta'^2}} \psi^> - \eta \partial_n \psi^> \right\} e^{-iKx} d\ell \quad (23)$$

with $k = +K$ for s_{10}^{+f} and $k = -K$ for s_{10}^{+b} .

At grazing incidence, since $s^+(k, k_0) = O(q_0)$, the limit

$$s_{01}^+(k) = \lim_{q_0 \rightarrow 0} \frac{s^+(k, k_0)}{q_0} \quad (24)$$

is finite. To compute this limit, let us divide Eq. (7) by q_0 et consider the limit when q_0 tends to zero. As mentioned earlier, the right-hand side has a finite limit. Therefore, $\psi_1^> = \lim_{q_0 \rightarrow 0} \frac{\psi^>}{q_0}$ and $\partial_n \psi_1^> = \lim_{q_0 \rightarrow 0} \frac{\partial_n \psi^>}{q_0}$ are solution of the same integral equations as $\psi^>$ and $\partial_n \psi^>$ but different right-hand side, allowing us to evaluate s_{01}^+ through Eq. (18)

$$s_{01}^+(k) = \frac{1}{\pi} \int_{\Gamma} \left\{ \left(\frac{ik\eta'\psi_1^>}{\sqrt{1 + \eta'^2}} - \partial_n \psi_1^> \right) \sin(q\eta) + \frac{q\psi_1^>}{\sqrt{1 + \eta'^2}} \cos(q\eta) \right\} e^{-ikx} d\ell \quad (25)$$

Finally, we can deduce the limit of the scattering amplitude when both incident and scattering angles go to grazing simultaneously,

$$s_{11}^+ = \lim_{q_0 \rightarrow 0, q \rightarrow 0} \frac{s^+(k, k_0)}{q_0 q} = \frac{1}{\pi} \int_{\Gamma} \left\{ \frac{ik\eta\eta' + 1}{\sqrt{1 + \eta'^2}} \psi_1^> - \eta \partial_n \psi_1^> \right\} e^{-ikx} d\ell \quad (26)$$

4. Numerical results

First, rough surfaces with both Gaussian height spectrum and Gaussian probability density function are studied, separating the air from glass with permittivity $\varepsilon = 2.37$. Two different kinds of roughness are investigated: small-scale or perturbative roughness with $\lambda/16$ height root mean square and $\lambda/2$ correlation length and resonance range roughness with $\lambda/4$ height root mean square and $\lambda/2$ correlation length.

Statistical NRCS is estimated through Monte Carlo average over 100 surface samples. Over the 42λ of the samples length, $\ell = 21\lambda$ have the roughness corresponding to the statistical parameters. On each side of the sample, there are 4.2λ -long smooth transition regions (see [13] for details) and 6.3λ -long plateaus. ℓ has to be set much larger than the larger scale of the roughness, that can be assumed to be the correlation length for Gaussian spectrum surfaces. Computing time for 100 samples at a given incidence angle is around 8 minutes, using MATLAB.

We start the numerical study with bistatic scattering, at an incidence angle of $\theta^i = 70^\circ$. For each surface sample, the scattering amplitude $s^+(k, k_0)$ for $k_0 = K \sin(\theta^i)$ is computed for all scattering directions $-K < k < +K$, as well as the limits $s_{10}^{+f}(k_0)$ and $s_{10}^{+b}(k_0)$. The rigorous NRCS $\sigma(k, k_0) = \text{Var}(s^+(k, k_0))$ can be compared to forward and backward extrapolations $q^2 \text{Var}(s_{10}^{+f}(k_0))$ and $q^2 \text{Var}(s_{10}^{+b}(k_0))$. As can be seen on Fig. 1, where the resonance range is addressed, the exact and extrapolated bistatic diagrams coincide over a range of 10 degrees from grazing. More precisely, in H-polarization, diagrams are closer than 1 dB up to -81° (-82° in V-pol.) for backward angles and up to -82° (-82° in V-pol.) in forward scattering.

We now focus on monostatic diagrams, that are of major importance for remote sensing. We compare in Figs. 2 and 3 the rigorous backscattering NRCS $\sigma^b(k_0) = \text{Var}(s^+(-k_0, k_0))$, at angles $70^\circ, 75^\circ, 80^\circ, 85^\circ, 87^\circ, 88^\circ$ and 89° , to the extrapolated diagram $q_0^4 \text{Var}(s_{11}^+)$. Note that the computing time for the extrapolated diagram is the same as for one incidence angle. Once again, the angle that corresponds to an error of 1 dB between exact and extrapolated diagrams appears on these figures. In order to determine this angle $\theta_{1 \text{ dB}}$ more precisely, the ratio $\sigma^b(k_0)/q_0^4$ is interpolated linearly between the monostatic

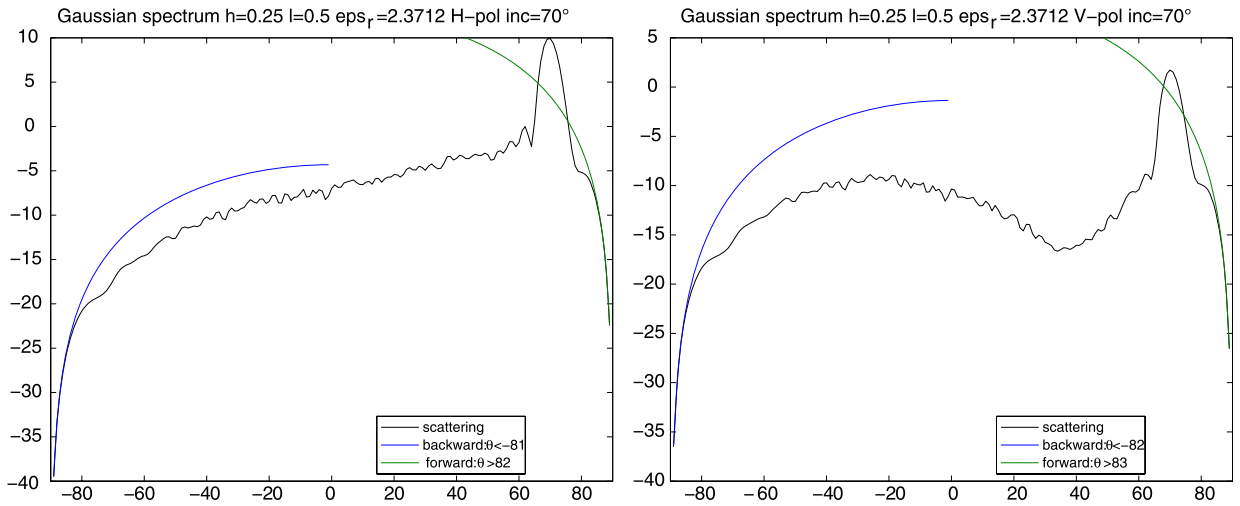


Fig. 1. 1D surface with Gaussian spectrum, $\lambda/4$ height root mean square and $\lambda/2$ correlation length, between air and glass $\varepsilon = 2.37$. Bistatic NRCS at 70° incidence.

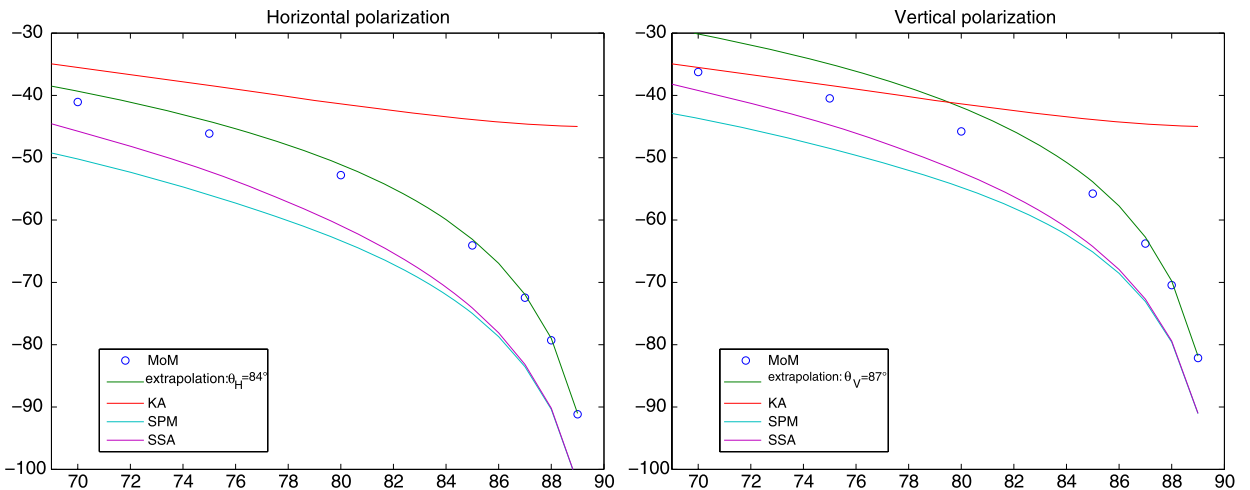


Fig. 2. 1D surface with Gaussian spectrum, $\lambda/16$ height root mean square and $\lambda/2$ correlation length, between air and glass $\varepsilon = 2.37$. Monostatic NRCS.

angles $70^\circ, 75^\circ, \dots, 89^\circ$, and finally compared, in dB, to $\text{Var}(s_{11}^+)$. As it can be seen, the value of this 1 dB angle barely depends on the roughness, being simply 85° in H-pol. and 87° in V-pol. For smaller angles, the behavior of the diagrams varies with both roughness and polarization. Note that in the case of the small roughness at H-pol., the extrapolation error is smaller than 3 dB as far as the incidence angle remains smaller than 70° .

The NRCS predicted by SPM and SSA at first order and KA also appear in Figs. 2 and 3. Those NRCS are computed via Monte Carlo averages, even if statistical expressions exist. This way, the same rough surface samples are used for all models, and the discrepancy between plots is only due to the physical approximations. Without surprise, the most problematic method is the KA, of which NRCS does not even tend toward zero at grazing, whatever the polarization. SPM and SSA largely underestimate the surface NRCS at all studied angles. Over the last grazing degrees, the error is 10 dB in Fig. 2, and much larger in Fig. 3. As expected, SSA and SPM curves coincide at grazing, and at large angles, SSA outperforms SPM.

For dielectric surfaces, the influence of the geometrical parameters on the accuracy of the extrapolated NRCS is thus quite moderate. We now turn to conducting media, with complex relative permittivity $\varepsilon = 30 + 30i$. Note here that the skin depth in the medium is very small compared to the electromagnetic wavelength in the vacuum, and the Grazing Method of Moments is applied under the curved surface-impedance approximation [15], using Eqs. (12) and (13). The same two kinds of roughness as previously are addressed, with surface samples of similar characteristics, except that the roughest surface has a correlation length of $3\lambda/4$ instead of $\lambda/2$, at monostatic angles $60^\circ, 80^\circ, 85^\circ, 89^\circ$. NRCS are compared in Figs. 4 and 5. For such a medium, a polarization effect appears clearly. In Horizontal polarization, extrapolation remains as accurate as for glass, by far outperforming the approximate models. However, in Vertical polarization, the GMoM and extrapolated curves coincide only at 89° , the error reaching 4 dB as soon as 85° is reached. This strong difference can be understood by noticing

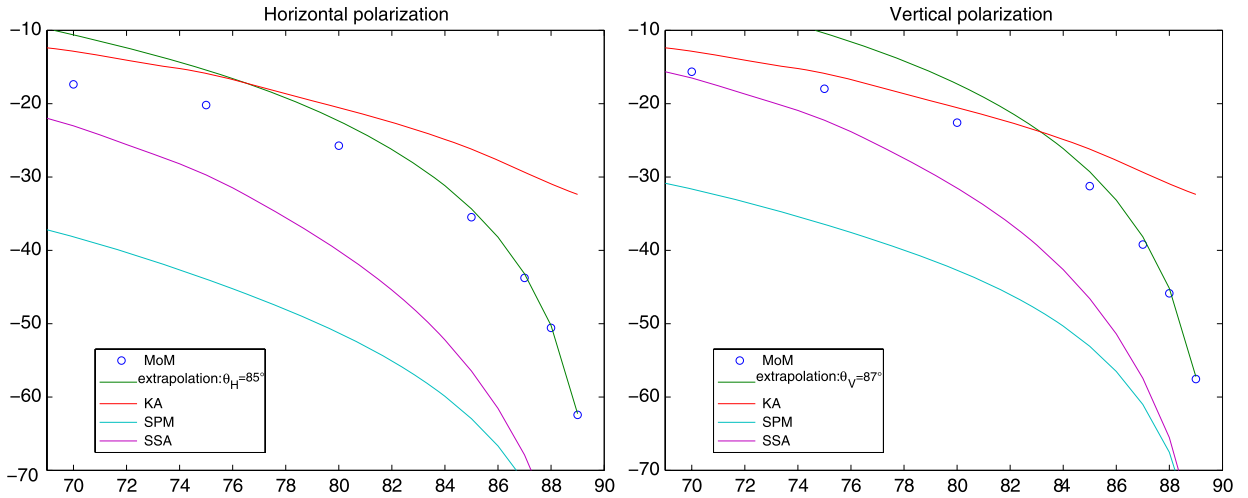


Fig. 3. 1D surface with Gaussian spectrum, $\lambda/4$ height root mean square and $\lambda/2$ correlation length, between air and glass $\epsilon = 2.37$. Monostatic NRCS.

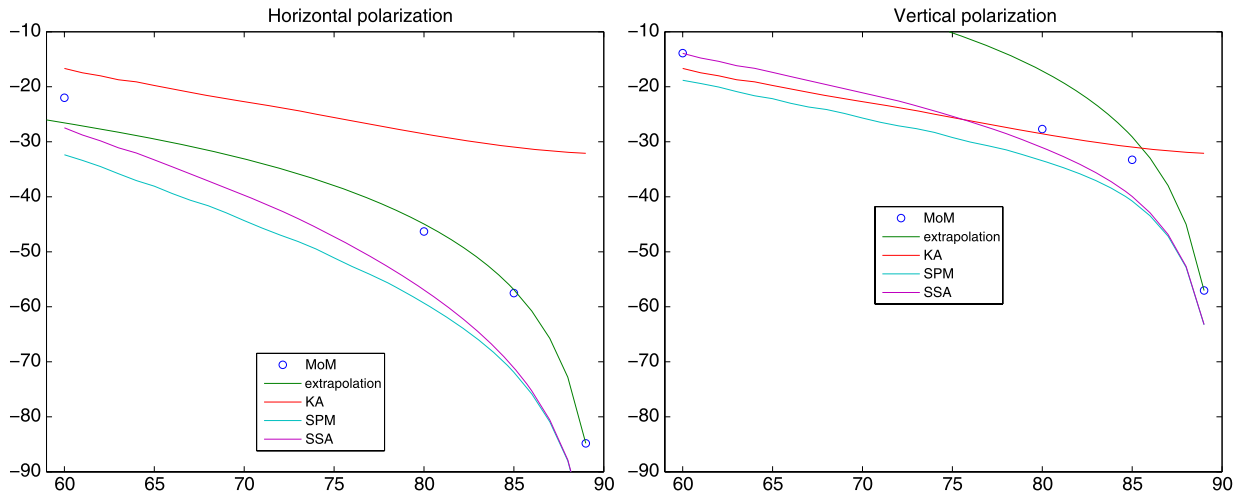


Fig. 4. 1D surface with Gaussian spectrum, $\lambda/16$ height root mean square and $\lambda/2$ correlation length, between air and conductor $\epsilon = 30 + 30i$. Monostatic NRCS.

that, in V polarization, the right-hand side of the integral Eq. (7) behaves as q_0 only at incidence angles larger than Brewster angle. For glass, it is about 57° , while for the conducting material considered here, it reaches 82° .

From 60° to 80° , SSA and KA show more accurate than the extrapolation, with errors smaller than 4 dB for small height roughness (Fig. 4). KA error is also smaller than 4 dB in the resonance range (Fig. 5).

The ocean surface exhibits a multiscale spectrum, including spatial frequencies from millimeter waves up to meter or decimeter waves, depending mainly on the wind speed. As such, it has scattering properties very different from surfaces with Gaussian spectrum. We consider for simulations the Unified ocean spectrum [14] for two different wind speeds (measured at a 10 m height), 4 m/s and 7 m/s and at L-band, that is with an electromagnetic wavelength of $\lambda = 25$ cm. For the 4 m/s wind speed case, the sea surface peak wave wavelength is 15 m, and the 100 surface samples are taken $\ell = 64$ m-long, with on each side a 1.6 m plateau and a 6.4 m transition region. Computation time reaches 90 minutes for each incidence angle $70^\circ, 75^\circ, 80^\circ, 85^\circ, 87^\circ, 88^\circ$ and 89° . For the 7 m/s wind speed case, the peak wave wavelength rises to 45 m, and all surface samples dimensions are increased fourfold, resulting in a 14 hours per incidence angle computing time. At L-band frequency, the ocean is a good conductor, and permittivity $\epsilon = 30 + 30i$ is set. Note that the generated surface samples are of Gaussian probability density function, which may be an important approximation for ocean surface remote sensing. As can be seen in Fig. 6 that displays the ocean NRCS against monostatic angle for the weaker wind speed, results are very polarization dependent. In the Horizontal case, extrapolation error is 1 dB at 82° and only 3 dB at 70° , while SPM and SSA are 4 dB away from GMoM at 70° , but the error of those approximate models is growing at grazing, reaching 8 dB from GMoM at 89° . On the contrary, for the Vertical polarization, from 70° up to 89° , SPM and SSA fit GMoM with a maximum

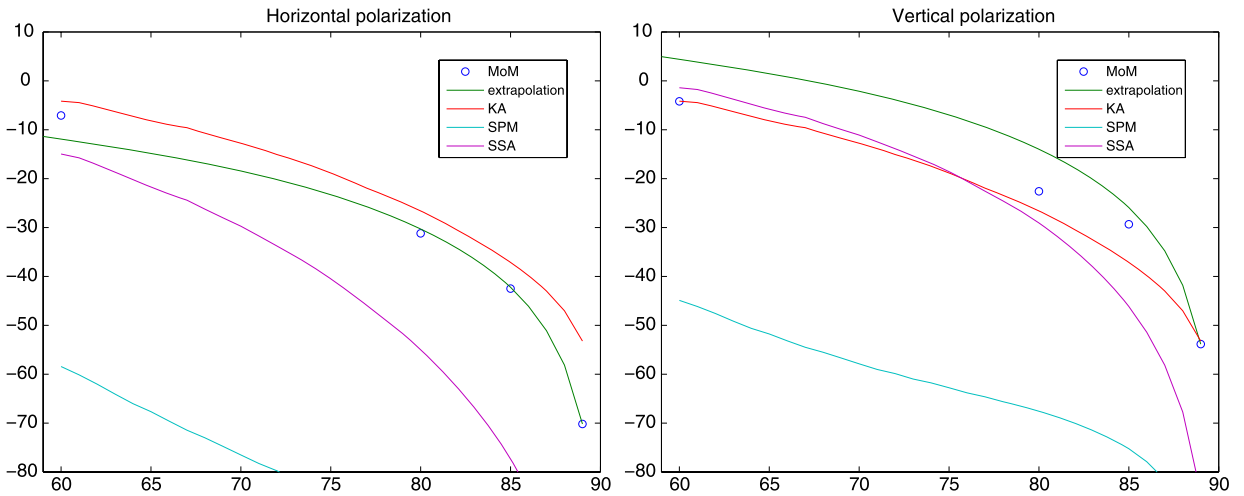


Fig. 5. 1D surface with Gaussian spectrum, $\lambda/4$ height root mean square and $3\lambda/4$ correlation length, between air and conductor $\epsilon = 30 + 30i$. Monostatic NRCS.

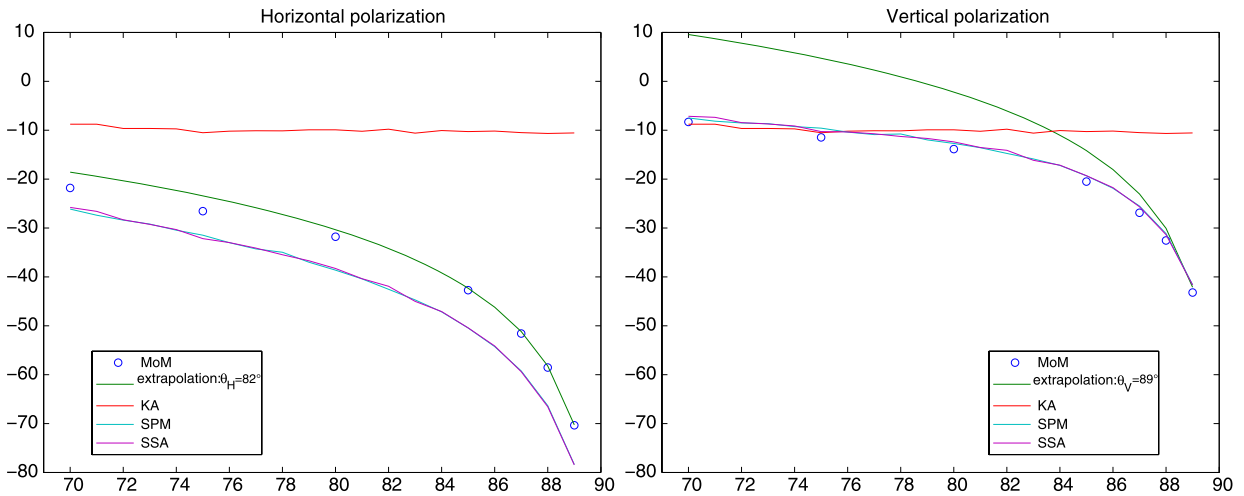


Fig. 6. 1D surface with Unified ocean spectrum [14], wind speed 4 m/s at L-band, permittivity $\epsilon = 30 + 30i$. Monostatic NRCS.

error of about 1.5 dB, while the extrapolation technique can only be used over the two most grazing degrees, with an error reaching 6 dB at 85° and 18 dB at 70° .

Those results worsen with the wind speed getting higher (Fig. 7). Note that 7 m/s is the average wind speed over the world. Here, for the Vertical polarization, the 1 dB error is reached by extrapolation as early as 88° . In fact, the H extrapolation error at 7 m/s is very close to the V one at 4 m/s. Also, for Vertical polarization at 7 m/s, for the first time in this paper, there is a visible difference between GMoM and extrapolation at 89° . SPM and SSA remain with a maximum error of 1.5 dB up to 87° , and of 5 dB at 89° .

5. Conclusion

It has been developed a complete theory of wave scattering from rough surfaces at grazing incidence and scattering angles. The resulting integral equations can be numerically solved by classical techniques and the whole method is called GMoM for Grazing Method of Moments. The paper is entirely focused on one-dimensional surfaces, but covers all common materials, dielectrics and conductors, that can be modeled by a complex permittivity.

From the integral relationship between the scattering amplitude and the solution of the GMoM, it has been shown how the scattering amplitude can be extrapolated in the LGA domain. Then from a single rigorous computation at one single incident angle, one can derive a monostatic diagram over a more or less extended part of the grazing angles.

We have performed some numerical computations to illustrate the performances of the theory and to derive the angular domain of validity of the presented extrapolation technique. For surfaces with Gaussian roughness spectrum, numerical

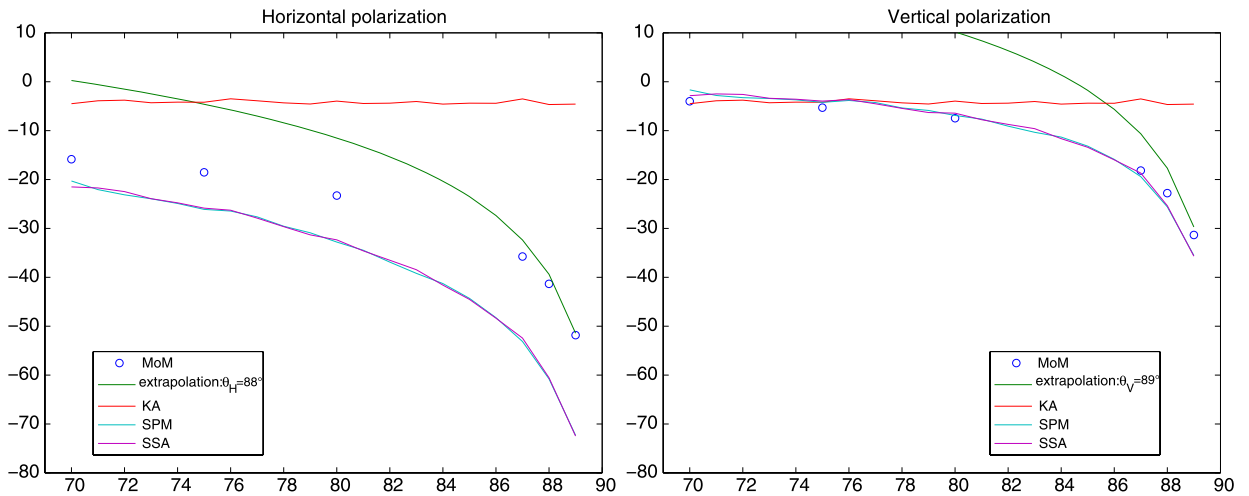


Fig. 7. 1D surface with Unified ocean spectrum [14], wind speed 7 m/s at L-band, permittivity $\epsilon = 30 + 30i$. Monostatic NRCS.

results indicate an important sensitivity to the nature of the lower medium, rather than to the roughness parameters. For dielectrics such as glass, the extrapolation is very accurate over the $[85^\circ; 90^\circ]$ angular range, whatever the polarization and the roughness, with maximum error around 1 dB, and it should always be preferred to elementary approximate models over those angles. However, for less grazing angles, no general rule obviously prevails. For conducting surfaces under Horizontally polarized illumination, the same accuracy and recommendations are true over $[85^\circ; 90^\circ]$; furthermore, extrapolation is meaningful at least up to 60° , with maximum errors around 4 dB. On the contrary, for conducting surfaces in the Vertical case, approximate models are to be chosen for angles smaller than 80° , and larger incidence angles than Brewster angle are required for accurate extrapolation.

The ocean surface at microwave, that has naturally only be investigated as a conductor, shows results highly depending on the wind speed. For calm seas (4 m/s wind speed), the conclusion is clear: there exists an easy way to accurately forecast the sea NRCS over the $[60^\circ; 90^\circ]$. One will rely on extrapolation for the H-NRCS, while SSA or SPM, the two methods coinciding here, will be trusted for the V case. Things get quickly more complex for moderate seas (7 m/s wind speed), where no method prevails in H, except extrapolation over $[85^\circ; 90^\circ]$, while in V, SSA and SPM keep great accuracy over $[60^\circ; 85^\circ]$, and no method performs better than 1 dB over $[85^\circ; 90^\circ]$. This last feature may in our opinion become more pronounced yet with stronger winds.

Admittedly, all those results have to be validated and backed up by 3D vector computations before being applied to natural surfaces. Cross-polarizations have also to be investigated. However, we have clearly stated that rigorous computations can be performed at the lowest grazing angles and can be used to generate monostatic diagrams as reference data. With our extrapolation technique, we prove that a simple approach can lead to accurate results in the difficult and complex domain of LGA.

References

- [1] G.S. Brown, Special issue on low-grazing-angle backscattering from rough surfaces, *IEEE Trans. Antennas Propag.* 46 (1998) 1–2.
- [2] T. Elfouhaily, C.A. Guérin, A critical survey of approximate scattering wave theories from random rough surfaces, *Waves Random Media* 14 (2004) R1–R40.
- [3] E. Thorsos, The validity of the Kirchhoff approximation for rough surface scattering using a Gaussian roughness spectrum, *J. Acoust. Soc. Am.* 83 (1988) 78–92.
- [4] E.I. Thorsos, The validity of the Kirchhoff approximation for rough surface scattering using a Gaussian roughness spectrum, *J. Acoust. Soc. Am.* A 82 (1989) 78–92.
- [5] E.I. Thorsos, S.L. Broshat, An investigation of the small-slope approximation for scattering from rough surfaces. Part II. Numerical studies, *J. Acoust. Soc. Am.* 101 (5) (1997) 2615–2625.
- [6] G. Soriano, C.-A. Guérin, M. Saillard, Scattering by two-dimensional rough surfaces: comparison between the method of moments, Kirchhoff and small-slope approximations, *Waves Random Media* 12 (2002) 63–83.
- [7] A.G. Voronovich, Small-slope approximation for electromagnetic wave scattering at a rough interface of two dielectric half-spaces, *Waves Random Media* 4 (1994) 337–367.
- [8] A. Ishimaru, J.D. Rockway, Y. Kuga, Rough surface Green's function based on the first-order modified perturbation and smoothed diagram methods, *Waves Random Media* 10 (2000) 17–31.
- [9] A. Ishimaru, J.D. Rockway, Y. Kuga, S.-W. Lee, TE and TM Green's function for coherent and incoherent propagation over a finitely conducting rough surface, *Radio Science* 37 (2002) 1–13.
- [10] H. Braunisch, Y. Zhang, C.O. Ao, S.E. Shih, Y.E. Yang, K.H. Ding, J.A. Kong, Tapered wave with dominant polarization stat for all angles of incidence, *IEEE Trans. Antennas Propag.* 48 (2000) 1086–1096.
- [11] D. Holliday, L.L. DeRaad, G.J. St-Cyr, Forward-backward: a new method for computing low-grazing angle scattering, *IEEE Trans. Antennas Propag.* 44 (1996) 722–729.

- [12] D.A. Kapp, G. Brown, A new numerical method for rough surface scattering calculations, *IEEE Trans. Antennas Propag.* 44 (1996) 711–721.
- [13] P. Spiga, G. Soriano, M. Saillard, Scattering of electromagnetic waves from rough surfaces: a boundary integral method for low-grazing angles, *IEEE Trans. Antennas Propag.* 56 (2008) 2043–2050.
- [14] T. Elfouhaily, B. Chapron, K. Katsaros, D. Vandemark, A unified directional spectrum for long and short wind-driven waves, *J. Geophys. Res.* 102 (C7) (July 1997) 15781–15796.
- [15] Marc Saillard, Daniel Maystre, Scattering from metallic and dielectric rough surfaces, *J. Opt. Soc. Amer. A* 7 (6) (1990) 982–990.
- [16] V.I. Tartarskii, M. Charnotskii, On the universal behavior of scattering from a rough surface for small grazing angles, *IEEE Trans. Antennas Propag.* 46 (1998) 67–72.